SCIENCE CHINA
Information Sciences

April 2021, Vol. 64 140306:1–140306:16
https://doi.org/10.1007/s11432-020-3013-1

• RESEARCH PAPER •
Special Focus on Wireless Communications with Unmanned Aerial Vehicles (UAVs)

A large-scale clustering and 3D trajectory optimization approach for UAV swarms

Ting MA, Haibo ZHOU*, Bo QIAN & Aiyong FU

School of Electronic Science and Engineering, Nanjing University, Nanjing 210023, *China*

Received 1 April 2020/Revised 22 June 2020/Accepted 27 July 2020/Published online 5 March 2021

Abstract With the significant development of unmanned aerial vehicles (UAVs) technologies, a rapid increase on the use of UAV swarms in a wide range of civilian and emergency applications has been witnessed. However, how to efficiently network the large-scale UAVs and implement the swarms applications without infrastructure support in remote areas is challenging. In this paper, we investigate a hierarchal large-scale infrastructure-less UAV swarm scenario, where numerous UAVs surveil and collect data from the ground and a ferry UAV (Ferry UAV) is designated to carry back all their collected data. We can divide UAV swarms into different areas based on their geographic locations due to the wide range of surveillance. To improve data collection efficiency of Ferry UAV, we introduce a single super cluster head (Super-CH) UAV in each area which can be selected by the proposed modified k-means clustering algorithm with low latency. Then, we design an iterative approach to optimize the 3-dimensional (3D) trajectory of Ferry UAV such that its data collection mission completion time is minimized. Numerical results show the efficiency and low-latency of the proposed clustering algorithm, and the proposed 3D optimal trajectory design for large-scale UAV swarms data collection admits better performance than that with fixed altitude.

Keywords large-scale UAV swarms, clustering, super-CH selection, 3D trajectory design

Citation Ma T, Zhou H B, Qian B, et al. A large-scale clustering and 3D trajectory optimization approach for UAV swarms. Sci China Inf Sci, 2021, 64(4): 140306, https://doi.org/10.1007/s11432-020-3013-1

1 Introduction

With an explosive data demand for the next-generation wireless networks, i.e., fifth generation (5G) or beyond 5G (B5G), a rapid increase on the use of unmanned aerial vehicles (UAVs) has been witnessed [1]. Since terrestrial wireless networks are deployed at fixed locations, it inevitably brings some limitations in such as mobility and flexibility [2, 3]. To overcome such drawbacks, UAVs are introduced to enable terrestrial communications from the sky [4–7]. The UAV-enabled communications have attracted extensive research attentions in plenty of applications, such as traffic control, precision agriculture, search and rescue [6–8]. Under this framework, UAVs are employed as aerial base stations (BSs), relays, and access points (APs), to assist the wireless communications of ground stations (GSs), or as cellular users for communications [9]. Compared with traditional terrestrial communication, UAV-enabled communications are more flexible and swift to deploy for temporary events. Furthermore, the line-of-sight (LoS) communication model is more probably adopted, owing to the high altitude of UAVs [10–12].

The majority of existing UAV-enabled communication systems generally build connections between the UAV and GSs. However, in some scenarios, such as emergency response or disaster area, the terrestrial communication infrastructure may not easily be established instantly, or the existing GSs are affected. Then, UAV-based networks provide an alternative solution for emergency situations [13]. Recently, the UAV becomes more and more popular in the emergency communication systems during rescue [14]. UAVs can implement data collection and transmit collected data to the target. Comparing to one single UAV, a group of UAVs is able to extend the mission coverage and ensure a reliable ad-hoc network with enhanced operation performances [15]. Hence, we mainly consider large-scale UAV swarms in this paper.

* Corresponding author (email: haibozhou@nju.edu.cn)

For large-scale UAV swarms, an effective clustering can reduce the communication overhead, increase the scalability and maximize the throughput [16]. Specifically, UAV swarms are partitioned into small groups, called clusters, within which there are one cluster head (CH) and some cluster members (CMs). The CH is selected from all UAVs in swarms and the performance of cluster can be controlled by managing CH effectively and efficiently. Thus, it is of great significance to select proper CH in each cluster.

Nowadays, there have been various UAV clustering algorithms. Ref. [17] proposed a multi-parameter weighted clustering approach to enhance the stability and survival rate of the UAV network. In [18], the authors introduced a gray wolf based clustering method, which can ensure reliable information transmission. On basis of the glowworm swarm optimization, Ref. [19] presented an energy aware UAV clustering scheme to cope with routing instability from nodes mobility and battery residual energy. In [20], the authors adjusted the transmission power of UAVs to save the energy consumption during communication, and the k-means clustering algorithm was adopted for CH selection to enhance the cluster lifetime and reduce the routing overhead. Ref. [21] proposed a clustering algorithm to obtain an energy-efficient solution and reduce the network traffic, which makes use of the multi-objective particle swarm optimization algorithm. In [22], a low latency communication approach is given to determine the optimal number of CHs. When the CH needs to transmit data to others, low latency communications are desirable. Therefore, it is necessary to develop efficient cluster formation and CH selection mechanism to decrease the communication delay for the large-scale UAV swarms.

After UAVs have collected data from the ground, they need to transmit their data to the ferry UAV (Ferry UAV), and the Ferry UAV then transmits its data collected from UAVs to a central controller. After CH UAVs are selected, the Ferry UAV can only collect data from each CH, which can greatly reduce the energy and time exhaustion for the Ferry UAV. To enhance communication performance, the trajectory of Ferry UAV can be designed optimally due to its controllable high mobility. There have been many studies about trajectory optimization recently [23–28]. Zeng et al. [23] jointly optimized the transmit power and trajectory to maximize the throughput in a UAV-enabled relaying system with the aid of block coordinate descent (BCD) technique. Wu et al. [24] jointly optimized the UAV trajectory and resource allocation to maximize the minimum average throughput of all users in UAV-enabled orthogonal frequency-division multiple access systems. Zhang et al. [25] maximized the average secrecy rates of the UAV-to-ground and ground-to-UAV transmissions by jointly optimizing the trajectory of the UAV and the transmit power of the legitimate transmitter. When coping with the nonconvex trajectory optimization, they exploited the successive convex approximation (SCA) technique. These techniques are usually used in UAV-enabled wireless communications [26–30]. Notice that, all these studies are argued in an assumption that the UAV is flying at a fixed altitude, which thereby is reduced to a 2-dimensional (2D) trajectory optimization. In practical applications, the Ferry UAV is able to change its altitude in real time. Meanwhile, when the Ferry UAV collects data from nodes with different altitudes, the efficiency of the Ferry UAV will decrease a lot if hovering a fixed altitude, especially when the heights of nodes vary widely. Hence, there is a need to design a 3D trajectory optimization of the Ferry UAV, which gives another main motivation of the current work.

In this paper, we study the data collection of large-scale UAV swarms as shown in Figure 1, where numerous UAVs collect data from different areas in layer 1 and the Ferry UAV gathers data from these UAVs in layer 2. On one hand, Some UAV swarms are wide apart and the number of UAVs is quite large, it is unaffordable for Ferry UAV to collect data from each UAV. Meanwhile, data collection in large-scale UAV swarms is transmission-delay sensitive. On the other hand, since the UAV swarms usually collect data in different areas, which may have different altitudes, then the efficiency of conventional 2D path planning with a fixed altitude of Ferry UAV will decrease a lot if the altitudes of areas vary widely. These motivate us to implement the clustering process in layer 1, and optimize a 3D trajectory of Ferry UAV in layer 2. Specifically, our main contributions can be summarized as follows.

(1) We propose a novel hierarchal and self-organized network structure for large-scale UAV swarms, in which UAVs can be dynamically managed in a cluster and a ferry UAV is efficiently designed to implement the data collection mission in remote emergency applications.

(2) We derive the optimal number of CHs in each area to minimize the transmission delay by means of queuing theory. Furthermore, to quickly select CHs and Super-CHs for the large-scale UAV swarms, we develop a modified k-means algorithm for the clustering design with low-complexity.

(3) Different from the existing 2D trajectory design solutions, we propose an iterative approach to optimize the 3D trajectory of the Ferry UAV by leveraging the BCD and SCA technologies, which is more suitable to the 3D UAV swarms emergency applications.

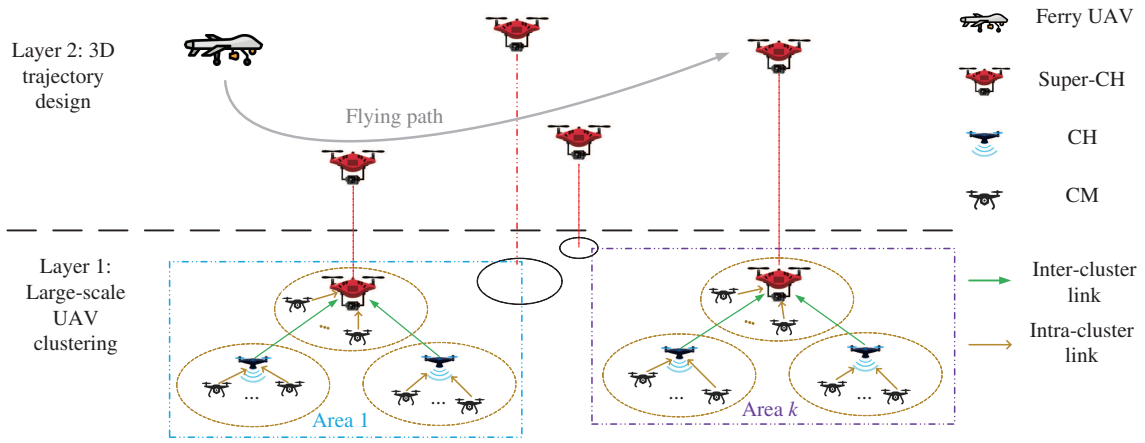

Figure 1 (Color online) Hierarchical framework for large-scale UAV clustering and 3D trajectory design in UAV swarms.

Table 1 Main notations

Notation	Meaning	Notation	Meaning
K	Total number of Super-CH UAVs (i.e., the number of areas)	$\alpha_i(t)$	Fraction of total bandwidth allocated for Super-CH i
M_k	Total number of UAVs in area k	B	Total available bandwidth
m	Packet size	P_i	Transmit power of Super-CH i
μ	Transmission rate of each UAV	$R_i(t)$	Instantaneous normalized achievable rate
T_t	Total transmission delay of each UAV	γ_0	Reference signal-to-noise ratio (SNR) at the reference distance of $d_0 = 1$ m
T_m	CM delay	C_i	Throughput requirement for Super-CH i
T_h	CH delay	N	Time slot number
$\boldsymbol{x}_i$, $\boldsymbol{s}_i$	Locations of UAVs and the Super-CH, respectively	δ	Length of time step
$\mathcal{C}_i$	Cluster i composed of CMs and one CH	$T_{\rm tr}$	Ferry UAV' traveling time
$\mathcal{U}$	Set of Super-CH UAVs	$\hat{\pi}$	Visiting order under TSP
$\boldsymbol{q}(t)$	Ferry UAV's trajectory	$T_{\rm tsp}$	Minimum traveling time under TSP
$V_{\max}$	Maximum Ferry UAV speed	$\bar{T}_i$	Time for Ferry UAV to satisfy the throughput requirement of Super-CH i
$d_{\min}$	Minimum safe distance between the Ferry UAV and Super-CH UAVs	$\tilde{T}_i$	Residence time of Ferry UAV at Super-CH i
$d_i(t)$	Distance between Ferry UAV and Super-CH i	r	Radius of the sphere centered at Super-CH
$h_i(t)$	Channel power gains	$\boldsymbol{g}_i$	Waypoint inside the sphere for Super-CH i

The rest of this paper is presented as follows. In Section 2, we give the problem description. In Section 3, the optimal number of CHs in each area is obtained by optimizing the transmission delay, and we propose a modified k-means algorithm to select the corresponding Super-CH selection of each area. The 3D trajectory optimization of the Ferry UAV based on BCD and SCA techniques is shown in Section 4. In Section 5, we present some numerical experiments to evaluate the performance, and we conclude the paper in Section 6.

We show the main notations used in this paper in Table 1, and denote scalars and vectors as italic letters and bold-face lower-case letters, respectively. Let $\mathbb{R}^n$ be the space of n-dimensional real vectors. For a vector $\boldsymbol{x} \in \mathbb{R}^n$, define its Euclidean norm as $\|\boldsymbol{a}\|$. Define $\log_2(\cdot)$ as the logarithm with base 2. Define $\dot{\boldsymbol{q}}(t)$ as the first-order derivative of a time-varying function $\boldsymbol{q}(t)$ with respect to time t.

2 Problem description

Consider a hierarchal large-scale UAV swarm scenario, where numerous UAVs collect data from different areas in layer 1 and the Ferry UAV gathers data from these UAVs in layer 2. Since there are numerous UAVs in each area, it is challenging for a Ferry UAV to collect data from each UAV. To address this issue, for layer 1, the UAVs that collect data from the ground are clustered and all of collected data are

gathered by one Super-CH within each area. As a result, in layer 2, the Ferry UAV only needs to collect data from these selected Super-CH. Suppose that the CMs in the same cluster communicate directly through one hop, and there is no collision between UAVs.

Assume that the large-scale UAV swarms are divided into K areas based on the geographic location, where there are M_k UAVs to collect data from the ground in area k, $k = 1, \ldots, K$. In layer 1, for area k, we first cluster M_i UAVs to several clusters with each cluster consisting of a CH and some CMs, and each CM transmits data to its CH in each cluster; then we select a CH as the Super-CH to gather data of all other CHs in each area. Under this setup, the Ferry UAV only needs to collect data from K Super-CHs. In layer 2, we design a 3D trajectory of the Ferry UAV to minimize the traveling time among the Super-CHs. Therefore, in the sequel, we will discuss how to select Super-CH in each area and design an optimal 3D trajectory of the Ferry UAV based on positions of selected Super-CHs.

3 Clustering and Super-CH selection

In this section, we first determine the number of CH UAVs such that the transmission delay of each area is minimized. Then, based on the optimal number of CHs in each area, we propose a modified k-means algorithm to select CHs and pick one CH as the corresponding Super-CH. We only analyze clustering and Super-CH selection in one area detailedly, which is easily extended to other areas.

3.1 Number of CHs

Supposing that there are M UAVs in an area, each UAV sends a packet with m bits, and its transmission rate is μ bps. When clustering is finished, there only exist data transmission between each CM and its CH, and that between CHs and the unique Super-CH, while the Super-CH gathers the total messages of the area and waits for the Ferry UAV to collect. In each area, time division multiple access (TDMA) technology is adopted to guarantee the reliable data collection in a large-scale UAV swarm. Specifically, for the transmission between CMs and its CH within each cluster, the TDMA is used to avoid interference among CMs in one cluster; For the transmission between CHs and the Super-CH within each area, we also apply the TDMA to eliminate interferences among CHs. Notably, the CM to its CH transmission in different clusters can be simultaneously occurred at one time slot. Hence, CMs and CHs need queue up to transmit data, which leads to the transmission delay.

Denote the transmission delay between the CM and its CH and that between CHs and Super-CH as CM delay and CH delay, respectively. Intuitively, the larger number of clusters leads to fewer CMs and more CHs, which causes smaller CM delay and larger CH delay. Hence, we attempt to find an optimal cluster number such that the UAV's transmission delay is minimized. When computing the transmission delay of a UAV, it relies on whether the UAV is a CM or a CH. Therefore, we focus on the expected transmission delay of a UAV. Accordingly, the expected transmission delay T_t of a UAV can be expressed as the sum of CM delay T_m when the UAV is a CM and CH delay T_h when the UAV is a CH, that is, $T_t = T_m + T_h$. Next, we will show how to calculate T_m and T_h.

Suppose that the number of CHs is S in this area, and each cluster has the same number of UAVs. Then, it immediately follows that there are $\frac{M}{S}$ UAVs in each cluster, i.e., $\frac{M}{S} - 1$ CMs and one CH. Accordingly, the probability that a UAV is a CM can be formulated as $P_{\mathrm{CM}} = \frac{M-S}{M}$. Meanwhile, since the Super-CH is one of CHs in the area, the probability that a UAV becomes a CH transmitting data to the Super-CH is $P_{\mathrm{CH}} = \frac{S-1}{M}$.

For the CM transmission, overall $\frac{M}{S} - 1$ CMs need to be transmitted to the CH in the cluster, while each CM needs to transmit one packet with m bits to the CH with transmission rate μ bps. Then, the transmission delay of one CM is $\frac{m \cdot (\frac{M}{S} - 1)}{\mu}$. Similar to [22], the CM delay T_m when the UAV is a CM should be the transmission delay of each CM multiplying the probability that the UAV is a CM, which can be formulated as

$$T_m = \frac{m \cdot (\frac{M}{S} - 1)}{\mu} \cdot P_{\mathrm{CM}}. \tag{1}$$

Analogously, each CH needs to transmit $\frac{M}{S}$ packets to the Super-CH, and there are $S - 1$ CHs queuing for transmission. Hence, the CH transmission delay T_h when the UAV is a CH is the transmission delay

of each CH multiplying the probability that the UAV is a CH, which is given by

$$T_h = \frac{m \cdot \frac{M}{S} \cdot (S-1)}{\mu} \cdot P_{\mathrm{CH}}. \tag{2}$$

Consequently, the overall expected transmission delay T_t is reformulated as

$$T_t = T_m + T_h = \frac{m \cdot (\frac{M}{S} - 1)}{\mu} \cdot P_{\mathrm{CM}} + \frac{m \cdot \frac{M}{S} \cdot (S-1)}{\mu} \cdot P_{\mathrm{CH}}. \tag{3}$$

Substituting P_{CM} and P_{CH} into Eq. (3), we obtain the overall expected transmission delay of a UAV as

$$T_t = \frac{M(S-1)^2 + (M-S)^2}{MS} \cdot \frac{m}{\mu}. \tag{4}$$

Therefore, the optimal number of CHs in the area should minimize T_t.

Since m and μ are all constants, minimizing T_t about S is equivalent to optimize the following function:

$$F(S) = \frac{M(S-1)^2 + (M-S)^2}{MS}.$$

By taking derivations with respect to S, the first and second order derivatives of $F(S)$ are as follows:

$$F'(S) = \frac{(M+1)(MS^2 - M^2)}{M^2S^2}, \quad F''(S) = \frac{2MS + 2S}{S^4}.$$

Owing to $M > 0$ and $S > 0$, we have $F''(S) > 0$, which means $F(S)$ is a convex function. Thus, the optimal S should satisfy equation $F'(S) = 0$, i.e., $S = \sqrt{M}$. Since S should be an integer as the number of CHs, we use floor$(\cdot)$ function to round down a number into an integer. In conclusion, for an area with M UAVs, we can derive the optimal number of CHs is

$$S = \begin{cases} \hat{S}, & \text{if } F(\hat{S}) \leqslant F(\hat{S}+1), \\ \hat{S}+1, & \text{otherwise}, \end{cases} \qquad \hat{S} = \mathrm{floor}(\sqrt{M}). \tag{5}$$

3.2 CHs and the Super-CH selection

According to the Shannon formula, the closer the distance between UAVs, the better the communication delay and quality. Hence, for the large-scale UAV scenario, we attempt to establish an efficient clustering method to make the communication distance between UAVs smallest. In this subsection, after the optimal number of CHs is derived by Eq. (5), we propose a modified k-means algorithm to cluster the large-scale UAV swarms for each area, select the CH of each cluster, and then choose one CH as the Super-CH.

For a given sample set, the standard k-means algorithm aims at clustering them to a prescribed number of clusters, such that the samples in one cluster are distributed as close as possible, while the distance between clusters is as large as possible. Meanwhile, for the standard k-means algorithm, each center point of a cluster is regarded as the CH even though the center point is not a point of the sample set. In our text, we have to select the CH of each cluster among UAVs. Therefore, we set the UAV closest to the center point as the CH, which is the main modification of our proposed approach compared to the standard k-means algorithm.

Notice that, when collecting data during a short time period, we suppose that UAVs hover in a small region and thus their positions can be regarded as unchanged. Hence, we denote the locations of M UAVs in the area as $\mathcal{D} = \{\boldsymbol{x}_1, \boldsymbol{x}_2, \ldots, \boldsymbol{x}_M\}$, where $\boldsymbol{x}_i$ is not time-varying. Meanwhile, supposing that M UAVs are divided into S clusters, we define the k-th cluster as $\mathcal{C}_k$, which is composed of some CMs and one CH. Then, based on the idea of k-means algorithm [31], our goal is to minimize the square error E, which is defined as follows:

$$E = \sum_{i=1}^{S} \sum_{\boldsymbol{x} \in \mathcal{C}_i} \|\boldsymbol{x} - \boldsymbol{u}_i\|^2, \tag{6}$$

where $\boldsymbol{u}_i$ is the mean vector (also called as center point) of cluster $\mathcal{C}_i$ with $\boldsymbol{u}_i = \frac{1}{|\mathcal{C}_i|} \sum_{\boldsymbol{x} \in \mathcal{C}_i} \boldsymbol{x}$. According to [31], minimizing E is NP-hard. Nevertheless, the standard k-means algorithm is a suitable heuristic

iterative method for it. Therefore, for the large-scale UAV swarm scenario, we propose a modified k-means algorithm to select the CH of each cluster and the Super-CH of each area, as shown in Algorithm 1. Specifically, in each cluster, we choose the UAV closest to the mean vector as the CH; After all CHs are determined, we further compute the distance between adjacent CHs, and then pick the CH closest to other CHs as the Super-CH. Consequently, the Super-CH of each area is obtained, which is a key ingredient for later trajectory design of the Ferry UAV. It is worth noting that, once positions of UAVs change a lot, the corresponding CHs and Super-CH of each area should be updated by implementing Algorithm 1.

Algorithm 1 Modified k-means algorithm for each area

1: **Input:** UAV swarms $\mathcal{D} = \{\boldsymbol{x}_1, \boldsymbol{x}_2, \ldots, \boldsymbol{x}_M\}$, clusters number S from (5).
2: **Output:** locations of Super-CHs.
3: Randomly select S UAVs from $\mathcal{D}$ as the initial mean vectors $\{\boldsymbol{\mu}_1, \boldsymbol{\mu}_2, \ldots, \boldsymbol{\mu}_S\}$.
4: Initialize $\mathcal{C}_i = \emptyset, i = 1, \ldots, S$.
5: **for** $j = 1, 2, \ldots, M$ **do**
6: Calculate the distance between each UAV $\boldsymbol{x}_j$ and each mean vector $\boldsymbol{\mu}_i$ $(1 \leqslant i \leqslant S)$: $d_{ji} = \|\boldsymbol{x}_j - \boldsymbol{\mu}_i\|$;
7: Determine the cluster label of $\boldsymbol{x}_j$ based on the nearest mean vector: $\lambda_j = \arg\min_{i \in \{1,2,\ldots,S\}} d_{ji}$;
8: Divide $\boldsymbol{x}_j$ into the corresponding cluster: $\mathcal{C}_{\lambda_j} = \mathcal{C}_{\lambda_j} \cup \{\boldsymbol{x}_j\}$.
9: **end for**
10: **for** $i = 1, 2, \ldots, S$ **do**
11: Calculate the new mean vector: $\boldsymbol{\mu}_i' = \frac{1}{|\mathcal{C}_i|} \sum_{\boldsymbol{x}_i \in \mathcal{C}_i} \boldsymbol{x}$;
12: **if** $\boldsymbol{\mu}_i' \neq \boldsymbol{\mu}_i$ **then**
13: Update the current mean vector $\boldsymbol{\mu}_i$ to $\boldsymbol{\mu}_i'$;
14: **else**
15: Keep the current mean vector $\boldsymbol{\mu}_i$ unchanged;
16: **end if**
17: **end for**
18: **Stop the Loop (Step 5–17)** until all mean vectors are not updated.
19: Select UAVs closest to the mean vector as the CHs.
20: Choose the CH closest to all other CHs as the Super-CH.

In the following section, according to the locations of selected Super-CHs, we will analyze how to design the optimal 3D trajectory of Ferry UAV such that its mission completion time is minimized, where the mission completion time refers to the time that Ferry UAV spends in finishing collecting data of all Super-CH UAVs.

4 3D trajectory optimization

4.1 Problem formulation

In our setup, the Ferry UAV is used as an aerial fusion center to collect data from Super-CHs which load all data transmitted by all other UAVs in the area. Inspired by [29], we aim to optimize the 3D trajectory of Ferry UAV according to the locations of Super-CHs selected in the above Section 3.

Since all UAVs are divided into K areas and each area has one Super-CH, then there are K Super-CHs, and the Super-CH set is defined by $\mathcal{U} = \{1, \ldots, K\}$. In general, the location of the Super-CH UAV is time-varying. However, since the flight area of the Super-CH UAV is not very wide, the Ferry UAV can wait for the Super-CH to fly back to its original position if the Super-CH has shifted to it at this time. Compared with the distance L between Super-CHs, the distance D between Super-CH's initial position and its current position can be ignored here because of $D \ll L$. Thus, we assume that the locations of Super-CHs are constant, without varying with time. For a given time horizon T, we denote the location of each Super-CH as $\boldsymbol{s}_i \in \mathbb{R}^3$, $i \in \mathcal{U}$, $0 \leqslant t \leqslant T$. Meanwhile, denote the Ferry UAV trajectory as $\boldsymbol{q}(t) \in \mathbb{R}^3$, $0 \leqslant t \leqslant T$. Correspondingly, the distance between Ferry UAV and Super-CH i is formulated as

$$d_i(t) = \|\boldsymbol{q}(t) - \boldsymbol{s}_i\|, \quad i \in \mathcal{U}. \tag{7}$$

Meanwhile, denote $V_{\max}$ as the maximum speed (m/s) of Ferry UAV. Then, we can easily obtain the constraint $\|\dot{\boldsymbol{q}}(t)\| \leqslant V_{\max}$, $0 \leqslant t \leqslant T$.

Observe that the communication link between Ferry UAV and Super-CHs is the UAV-UAV link. Taking the fading effect into account, the Rician fading model [10] is applied in the UAV-UAV link, where the involved Rician factor accounts for the influence of scattering and reflection from the surrounding environments. For the Rician fading model with a large Rician factor, it is properly approximated by the LoS channel model [32]. On the other hand, when UAVs operate at sufficiently high altitudes, the

probability of LoS link is generally high. Therefore, in this paper, we assume that the uplink communications between the Ferry UAV and Super-CHs are LoS links. Meanwhile, according to [9], the UAV-UAV channel can be characterized by the simple free-space path loss model generally. Hence, the channel power gains follow from the free-space path loss model as

$$h_i(t) = \lambda_0 d_i(t)^{-2}, \quad i \in \mathcal{U}, \tag{8}$$

where λ_0 is the channel power gain at the reference distance of $d_0 = 1$ m and $d_i(t)$ represents the distance between Ferry UAV and Super-CH i defined by Eq. (7).

Denote the transmit power and the total available bandwidth of Super-CH i by P_i and B, respectively, $i \in \mathcal{U}$. Meanwhile, the Ferry UAV adopts frequency division multiple access (FDMA) scheme with dynamic bandwidth allocation among all Super-CHs, i.e., Ferry UAV could collect messages from multiple Super-CHs at one time slot. Denote $\alpha_i(t)$ as the fraction of the total bandwidth that is allocated for Super-CH i at time t, $i \in \mathcal{U}$. Accordingly, for $\alpha_i(t)$, we can get the constraints as follows:

$$\sum_{i=1}^{K} \alpha_i(t) \leqslant 1, \quad \alpha_i(t) \geqslant 0, \ \forall i, t. \tag{9}$$

It is worth noting that the dynamic FDMA scheme involves FDMA with fixed user bandwidth allocation and TDMA with dynamic user time scheduling as special cases. Specifically, it becomes the dynamic TDMA scheme with $\alpha_i(t)$ being binary variable, while we obtain the non-dynamic FDMA scheme with $\alpha_i(t) = \alpha_i$, $\forall t$.

Subsequently, when Super-CH i transmits data to the Ferry UAV (i.e., $\alpha_i(t) > 0$), we formulate its instantaneous normalized achievable rate in bits/second/Hertz (bps/Hz) as

$$\tilde{R}_i(t) = \alpha_i(t) \log_2 \left(1 + \frac{P_i h_i(t)}{\alpha_i(t) B N_0}\right) = \alpha_i(t) \log_2 \left(1 + \frac{P_i \gamma_0}{\alpha_i(t) \|\boldsymbol{q}(t) - \boldsymbol{s}_i\|^2}\right), \tag{10}$$

where N_0 denotes the additive white Gaussian noise (AWGN) power spectral density in watts/Hz, while $\gamma_0 \triangleq \lambda_0/(BN_0)$ represents the reference SNR at reference distance of $d_0 = 1$ m. When Ferry UAV is close to Super-CH i at time t, i.e., $\boldsymbol{q}(t) \to \boldsymbol{s}_i$, Eq. (10) implies that the instantaneous normalized achievable rate $\tilde{R}_i(t) \to \infty$, which is obviously not realistic. Meanwhile, the distance between the Super-CH UAV should be larger than a prescribed safe distance due to collision avoidance. Therefore, we modify the instantaneous normalized achievable rate of Super-CH i as follows:

$$R_i(t) = \alpha_i(t) \log_2 \left(1 + \frac{P_i \gamma_0}{\alpha_i(t) \max(\|\boldsymbol{q}(t) - \boldsymbol{s}_i\|^2, d_{\min}^2)}\right), \tag{11}$$

where $d_{\min}$ is the minimum safe distance between Ferry UAV and Super-CHs to ensure collision avoidance.

Suppose that the Ferry UAV only executes data collection once by one single fly mission. It is reasonable in many practical applications, for instance, the service requests of Super-CHs are intermittent. Then, Ferry UAV mission is finished once the throughput of each Super-CH meets its target requirement. Denote the throughput requirement of Super-CH i as C_i bits, $i \in \mathcal{U}$. Moreover, define T as the mission completion time that Ferry UAV costs in finishing collecting data of all Super-CH UAVs.

With the aforementioned constraints, our goal is to minimize the mission completion time T via an optimal trajectory design. In fact, minimizing T is of great practical significance, which is beneficial for saving more time and energy for the Ferry UAV and avoiding large communication delay of Super-CH UAVs. For notation brevity, define $\mathcal{Q} \triangleq \{\boldsymbol{q}(t)\}$ and $\mathcal{A} \triangleq \{\alpha_i(t)\}$. According to the above arguments, we aim to minimize the completion time T by jointly optimizing the Ferry UAV's trajectory $\mathcal{Q}$ and the bandwidth allocation $\mathcal{A}$, with satisfying the throughput requirements of all Super-CHs. As a result, the optimization problem is written as

$$\begin{aligned}
(\mathrm{P1}) \quad & \min_{T, \mathcal{Q}, \mathcal{A}} \quad T \\
& \text{s.t.} \quad B \int_0^T R_i(t) \mathrm{d}t \geqslant C_i, \ \forall i, && (12) \\
& \qquad \sum_{i=1}^{K} \alpha_i(t) \leqslant 1, \quad \alpha_i(t) \geqslant 0, \ \forall i, t, && (13)
\end{aligned}$$

$$\|\dot{\boldsymbol{q}}(t)\| \leqslant V_{\max},\ \forall t,\quad \boldsymbol{q}(0)=\boldsymbol{q}(T), \tag{14}$$

where $R_i(t)$ is given by Eq. (11). Note that in problem (P1), we impose an extra constraint (14) on Ferry UAV's initial and final locations, i.e., the Ferry UAV should return to its initial location after finishing the data collection. It is meaningful in practical scenarios such as periodical data collections [29]. Due to the linearity of the constraint on Ferry UAV's initial and final locations, follow-up results are not difficult to be extended to cases without such constraints correspondingly.

Obviously, variables $\mathcal{Q}$ and $\mathcal{A}$ in Problem (P1) are infinite-dimensional due to the continuous time t. Meanwhile, $R_i(t)$ in constraint (12) is not concave with respect to $\boldsymbol{q}(t)$, which leads to the nonconvexity of problem (P1). In addition, the variable T is involved as the upper bound of integration interval in constraint (12), so the corresponding integration lacks a closed-form expression. Therefore, problem (P1) is generally challenging to cope with directly. In the sequel, we will refer to analyses in [29] to approximately solve problem (P1).

4.2 Problem solution

Since variables T, $\boldsymbol{q}(t)$ and $\alpha_i(t)$ are closely coupled with each other, we introduce an intermediate variable η for problem (P1) such that variables T and $\{\boldsymbol{q}(t),\alpha_i(t)\}$ can be optimized sequentially. For a given T, consider the following optimization problem

$$\begin{aligned}(\text{P1.1})\quad \max_{\eta,\mathcal{Q},\mathcal{A}}\ & \eta\\ \text{s.t.}\ & \frac{B}{C_i}\int_0^T R_i(t)\mathrm{d}t \geqslant \eta,\ \forall i,\\ & \sum_{i=1}^{K}\alpha_i(t)\leqslant 1,\quad \alpha_i(t)\geqslant 0,\ \forall i,t,\\ & \|\dot{\boldsymbol{q}}(t)\|\leqslant V_{\max},\ \forall t,\quad \boldsymbol{q}(0)=\boldsymbol{q}(T).\end{aligned} \tag{15}$$

Assume that the optimal solution of problem (P1.1) is $\eta^*(T)$. Then, constraint (12) of problem (P1) is naturally equivalent to $\eta^*(T)\geqslant 1$. As a consequence, problem (P1) is equivalently transformed into

$$\begin{aligned}(\text{P1.2})\quad \min_{T}\ & T\\ \text{s.t.}\ & \eta^*(T)\geqslant 1.\end{aligned} \tag{16}$$

Notably, as T increases, it is easy to deduce from constraint (15) that the constraint set of η becomes wider. Then, the optimal objective function value $\eta^*(T)$ gets larger. Hence, we provide the following lemma without proof.

Lemma 1. The optimal solution $\eta^*(T)$ of problem (P1.1) is a non-decreasing function of T.

According to the monotonicity of $\eta^*(T)$ in Lemma 1, the optimal solution T^* of problem (P1.2) should satisfy $\eta^*(T^*)=1$. Meanwhile, once $\eta^*(T)$ can be obtained for any given T, we are able to apply the bisection method to efficiently search T satisfying $\eta^*(T)=1$. Thus, our efforts are devoted to solve problem (P1.1) to get $\eta^*(T)$ for given T.

For the convenience of analyses on problem (P1.1), we discretize the time horizon T into N time slots equally, where the corresponding time step $\delta=\frac{T}{N}$ is sufficiently small to let the distance between Ferry UAV and Super-CHs be approximately regarded as constant within each time step δ. Then, the time horizon T could be expressed as N time slots $[t_1,\ldots,t_N]$ with $t_n=n\delta$, $n=1,\ldots,N$. Accordingly, the trajectory $\boldsymbol{q}(t)$ of Ferry UAV over T can be discreted as $\boldsymbol{q}[n]=q(t_n)$, $n=1,\ldots,N$, while the Ferry UAV's speed is expressed as

$$\|\dot{q}(n)\|=\frac{\|\boldsymbol{q}[n+1]-\boldsymbol{q}[n]\|}{\delta},\quad n=1,\ldots,N-1.$$

Similarly, the bandwidth allocation could be discretized as $\alpha_i[n]=\alpha_i(t_n)$, the location of Super-CH i is $\boldsymbol{s}_i=\boldsymbol{s}_i(t_n)$, and the achievable rate between Super-CH i and the Ferry UAV at time slot n is thereby

$$R_i[n]=\alpha_i[n]\log_2\left(1+\frac{P_i\gamma_0}{\alpha_i[n]\max(\|\boldsymbol{q}[n]-\boldsymbol{s}_i\|^2,d_{\min}^2)}\right). \tag{17}$$

As a result, rewriting $\mathcal{Q}=\{\boldsymbol{q}[n]\}$ and $\mathcal{A}=\{\alpha_i[n]\}$, problem (P1.1) is reformulated as

$$\begin{aligned}(\text{P1.3})\quad &\max_{\eta,\mathcal{Q},\mathcal{A}}\ \eta\\ &\text{s.t.}\quad \frac{B\delta}{C_i}\sum_{n=1}^{N}R_i[n]\geqslant\eta,\ \forall i, &(18)\\ &\sum_{i=1}^{K}\alpha_i[n]\leqslant 1,\quad \alpha_i[n]\geqslant 0,\quad \forall i,n, &(19)\\ &\frac{\|\boldsymbol{q}[n+1]-\boldsymbol{q}[n]\|^2}{\delta^2}\leqslant V_{\max}^2,\quad n=1,\ldots,N-1,\quad \boldsymbol{q}[1]=\boldsymbol{q}[N], &(20)\end{aligned}$$

where constraints (18)–(20) correspond to discretizations of constraints (12)–(14) in problem (P1).

Despite that problem (P1.3) is non-convex, with fixed $\mathcal{Q}$, it is reduced to a convex problem with respect to $(\eta,\mathcal{A})$ (details are shown in the following Subsection 4.2.1). Then, for given $\mathcal{Q}$, variable $(\eta,\mathcal{A})$ can be directly obtained by CVX toolbox [33]. Meanwhile, when $\mathcal{A}$ is fixed, by leveraging on the SCA technique, problem (P1.3) can be relaxed to a convex programming as well, which is easily dealt with by CVX toolbox in MATLAB. It is noticed that the well-known BCD technique is a frequently used method to cope with a separately convex problem [29, 30, 34]. Following the similar idea in [29], we will adopt the BCD based algorithm to iteratively solve problem (P1.3), i.e., repeatedly and alternatively optimizing $(\eta,\mathcal{A})$ with fixed trajectory $\mathcal{Q}$ and $(\eta,\mathcal{Q})$ with fixed bandwidth allocation $\mathcal{A}$ until the value of η changes within a prescribed threshold.

4.2.1 *Bandwidth allocation optimization with fixed trajectory*

Suppose that the trajectory $\mathcal{Q}=\{\boldsymbol{q}[n]\}$ is fixed. Recalling the expression of $R_i[n]$ in Eq. (17), problem (P1.3) is reduced to

$$\begin{aligned}(\text{P1.4})\quad &\max_{\eta,\mathcal{A}}\ \eta\\ &\text{s.t.}\quad \frac{B\delta}{C_i}\sum_{n=1}^{N}\alpha_i[n]\log_2\left(1+\frac{P_i\gamma_0}{\alpha_i[n]z_i[n]}\right)\geqslant\eta,\ \forall i, &(21)\\ &\sum_{i=1}^{K}\alpha_i[n]\leqslant 1,\quad \alpha_i[n]\geqslant 0,\quad \forall i,n,\end{aligned}$$

where the term $z_i[n]\triangleq\max(\|\boldsymbol{q}[n]-\boldsymbol{s}_i\|^2,d_{\min}^2)$ is a constant with respect to $\alpha_i[n]$ and η for given $\mathcal{Q}=\{\boldsymbol{q}[n]\}$. Therefore, the LHS of (21) is a concave function of $\alpha_i[n]$. Combined with the linearity of the objective function and other constraints, we can deduce that problem (P1.4) is convex. Therefore, it can be easily solved by CVX toolbox in MATLAB.

4.2.2 *Trajectory optimization with fixed bandwidth allocation*

When $\mathcal{A}$ is given, problem (P1.3) is correspondingly transformed to

$$\begin{aligned}(\text{P1.5})\quad &\max_{\eta,\mathcal{Q}}\ \eta\\ &\text{s.t.}\quad \frac{B\delta}{C_i}\sum_{n=1}^{N}R_i[n]\geqslant\eta,\quad \forall i, &(22)\\ &\frac{\|\boldsymbol{q}[n+1]-\boldsymbol{q}[n]\|^2}{\delta^2}\leqslant V_{\max}^2,\quad n=1,\ldots,N-1,\quad \boldsymbol{q}[1]=\boldsymbol{q}[N],\end{aligned}$$

where $R_i[n]$ is given by Eq. (17). Note that, constraint (22) is not convex. However, it is not difficult to verify that $R_i[n]$ is a convex function of the term $\max(\|\boldsymbol{q}(t)-\boldsymbol{s}_i\|^2,d_{\min}^2)$. Hence, we are able to transform constraint (22) to a convex one by introducing a concave lower-bound of $R_i[n]$ with respect to $\boldsymbol{q}[n]$, similarly as in [29, 30]. For this purpose, we first propose the following result.

Lemma 2. For a given trajectory $\mathcal{Q}^l \triangleq \{\boldsymbol{q}^l[n]\}$, $R_i[n]$ can be lower bounded by $\hat{R}_i[n]$ with

$$\hat{R}_i[n] \triangleq \alpha_i[n]\log_2\left(1+\frac{P_i\gamma_0}{\alpha_i[n]z_i^l[n]}\right)-\phi_i^l[n](z_i[n]-z_i^l[n]), \tag{23}$$

where

$$z_i[n]=\max(\|\boldsymbol{q}[n]-\boldsymbol{s}_i\|^2,d_{\min}^2),\quad z_i^l[n]=\max(\|\boldsymbol{q}^l[n]-\boldsymbol{s}_i\|^2,d_{\min}^2),\quad \phi_i^l[n]=\frac{\alpha_i[n]P_i\gamma_0\log_2 e}{z_i^l[n](\alpha_i[n]z_i^l[n]+P_i\gamma_0)}.$$

Proof. Please refer to Appendix A.

It is easy to see from Lemma 2 that $R_i[n]\geqslant\hat{R}_i[n]$ and the equality holds if $\boldsymbol{q}^l[n]=\boldsymbol{q}[n]$. In addition, we can deduce the following results holds true.

Lemma 3. For a given local trajectory $\mathcal{Q}^l \triangleq \{\boldsymbol{q}^l[n]\}$, the lower bound $\hat{R}_i[n]$ defined in Eq. (23) is concave with respect to $\boldsymbol{q}[n]$.

Proof. Please refer to Appendix B.

According to Lemma 3, nonconvex constraint (22) in (P1.5) is transformed to a convex one. Hence, we can obtain a lower bound of the optimal value of problem (P1.5) via solving the approximate problem

$$\begin{aligned}(\text{P1.6})\quad &\max_{\eta,\mathcal{Q}}\ \eta\\ &\text{s.t.}\ \ \frac{B\delta}{C_i}\sum_{n=1}^{N}\hat{R}_i[n]\geqslant\eta,\ \forall i,\\ &\qquad\frac{\|\boldsymbol{q}[n+1]-\boldsymbol{q}[n]\|^2}{\delta^2}\leqslant V_{\max}^2,\quad n=1,\ldots,N-1,\quad \boldsymbol{q}[1]=\boldsymbol{q}[N].\end{aligned} \tag{24}$$

With convex objective function and convex constraints, problem (P1.6) is convex, which can be solved by standard convex optimization techniques such as the CVX toolbox [33]. Notice that, the optimal solution of problem (P1.6) is a lower bound of that of problem (P1.5). Therefore, we iteratively solve problem (P1.6) multiple times to improve the quality of the solution.

4.2.3 *Iterative bandwidth allocation and trajectory optimization*

According to the above arguments, we summarize the BCD based algorithm for approximately solving problem (P1.3) in Algorithm 2. Note that, (P1.4) and (P1.6) are convex, which are both solved optimally. Since the objective function value η of problem (P1.3) is monotonically non-decreasing in each iteration and upper bounded, then the sequence $\{\mathcal{Q}^l\}$ obtained by Algorithm 2 can converge to a locally optimal solution of problem (P1.3) following the analysis similar to [29].

Algorithm 2 BCD based algorithm for (P1.3)

Input: A given T, initial trajectory of the Ferry UAV $\mathcal{Q}^0$, prescribed thresholds $\epsilon_1>0$, $\epsilon_2>0$, $l=0$.
Output: $\mathcal{Q}^l$, $\mathcal{A}^l$, η^l.

while $\frac{\eta^{l+1}-\eta^l}{\eta^l}\geqslant\epsilon_2$ **do**
  For given $\mathcal{Q}^l$, obtain $\mathcal{A}^{l+1}$ by solving problem (P1.4);
  Initialize the inner iterative index $r=0$ and the inner initial trajectory $\mathcal{Q}^{l,0}=\mathcal{Q}^l$;
  while $\frac{\eta^{r+1}-\eta^r}{\eta^r}\geqslant\epsilon_1$ **do**
    For given $\mathcal{A}^{l+1}$ and $\mathcal{Q}^{l,r}$, obtain $\mathcal{Q}^{l,r+1}$ and η^{r+1} by solving problem (P1.6);
    $r=r+1$;
  end while
  $\mathcal{Q}^{l+1}=\mathcal{Q}^{l,r}$, $\eta^{l+1}=\eta^r$;
  $l=l+1$;
end while

The computational complexity of Algorithm 2 depends mainly on the resolutions of (P1.4) and (P1.6). Since problem (P1.4) and problem (P1.6) are both convex programmings with $KN+1$ variables, we can solve them by employing a primal-dual interior point method, whose computation complexity is $O((KN+1)^3\log(\epsilon^{-1}))$ with ϵ being the accepted duality gap. Supposing that the number of iterations in the outer and inner loops are L_1 and L_2 respectively, the total computation complexity for the BCD based algorithm can be calculated as $O((L_1+L_1L_2)(KN+1)^3\log(\epsilon^{-1}))$. Therefore, the proposed BCD based algorithm runs in a polynomial time.

4.3 TSP based initial trajectory design

For the proposed BCD based algorithm in Algorithm 2, its convergence results generally depend on the Ferry UAV trajectory initialization [29]. Thus, it is important to provide a proper initial trajectory of the Ferry UAV. In this section, we propose the TSP based 3D trajectory initialization referring to [29].

Recall that the location of Super-CH i is denoted as $\boldsymbol{s}_i \in \mathbb{R}^3$, $i \in \mathcal{U}$. We first determine the optimal visiting order of all Super-CHs by minimizing the traveling distance to visit all Super-CHs for the Ferry UAV. This is actually the classic traveling salesman problem (TSP) [35], which is NP-hard. Nevertheless, there exist various algorithms obtaining high-quality approximate solutions with an affordable computational time [35]. Subsequently, based on the locations of all Super-CHs, we acquire the minimum traveling time $T_{\rm tsp}$ and the optimal visiting order $\hat{\pi} \triangleq [\hat{\pi}(1), \ldots, \hat{\pi}(K)]$, where $\hat{\pi}(i)$ stands for the index of the Super-CH which is the i-th one to be visited.

Next, for a given flight time T, we will discuss how to generate a Ferry UAV's initial trajectory, which is partitioned into two cases depending on whether T is larger than $T_{\rm tsp}$, as follows.

4.3.1 *Case 1:* $T \geqslant T_{\rm tsp}$

In this scenario, T is larger than the $T_{\rm tsp}$, so the Ferry UAV can arrive at each Super-CH within T. Then, the remaining time $T - T_{\rm tsp}$ is spent by the Ferry UAV to stay around the Super-CHs. Assume that the Ferry UAV only collects data from Super-CH i when their distance attains the minimum safe distance, that is to say, Super-CH i only transmits data with the maximum instantaneous achievable rate. To determine the residence time allocation $\tilde{T}_i$ among Super-CH i, denote $\bar{T}_i$ as the time required for the Ferry UAV to satisfy the throughput requirement of Super-CH i. Then we obtain

$$\bar{T}_i = \frac{C_i}{B \log_2 \left(1 + \frac{P_i \gamma_0}{d_{\min}^2}\right)}, \quad \forall i. \tag{25}$$

Subsequently, the total residence time $T - T_{\rm tsp}$ can be proportionally divided among the Super-CHs. As a result, the residence time of Ferry UAV at Super-CH i $\tilde{T}_i$ can be formulated as

$$\tilde{T}_i = \frac{\bar{T}_i (T - T_{\rm tsp})}{\sum_{y=1}^{K} \bar{T}_y}, \quad \forall i \in \mathcal{U}. \tag{26}$$

Combining the optimal visiting order $\hat{\pi}$ with the residence time allocation in (26) for each Super-CH, we can obtain the initial trajectory $\mathcal{Q}_0$ in the case of $T \geqslant T_{\rm tsp}$ accordingly.

4.3.2 *Case 2:* $T < T_{\rm tsp}$

For this case, the Ferry UAV is not able to reach all Super-CHs. To construct a feasible initial trajectory, we first specify a spherical region for each Super-CH, which is centered at the corresponding Super-CH with radius r. Then, via designing the Ferry UAV trajectory and radius r properly, we hope to minimize the Ferry UAV traveling distance while the Ferry UAV is guaranteed to reach each spherical region. Similar to [29], the problem could be expressed as follows:

$$\begin{aligned} (\text{P2}) \quad & \min_{r, \boldsymbol{q}(t), T_{\rm tr}} \quad T_{\rm tr} \\ & \text{s.t.} \quad \min_{0 \leqslant t \leqslant T_{\rm tr}} \|\boldsymbol{q}(t) - \boldsymbol{s}_i\| \leqslant r, \quad \forall i \in \mathcal{U}, \qquad (27) \\ & \qquad \|\dot{\boldsymbol{q}}(t)\| \leqslant V_{\max}, \quad \forall 0 \leqslant t \leqslant T_{\rm tr}, \quad \boldsymbol{q}(0) = \boldsymbol{q}(T_{\rm tr}), \qquad (28) \end{aligned}$$

where constraint (27) ensures that all spheres for Super-CHs can be traversed by the Ferry UAV, because there exists at least one time instant t such that the distance between Ferry UAV and Super-CH i does not exceed r. For fixed radius r, define the optimal objective function value of (P2) by $T_{\rm tr}^*(r)$. We can easily deduce that $T_{\rm tr}^*(r)$ is a non-increasing function of r. Therefore, we turn to solve (P2) with a fixed r to obtain the corresponding $T_{\rm tr}^*(r)$, and then adopt the bisection method to search for the optimal r^* such that $T_{\rm tr}^*(r^*) = T$. Next, we convert to solving (P2) with arbitrary fixed radius r.

Based on Lemma 2 in [29], the optimal trajectory $\boldsymbol{q}(t)$ in problem (P2) only contains connected line segments. Thus, for arbitrary given r, we can reduce problem (P2) to optimizing waypoints inside spheres,

which are actually the starting and ending points of line segments, and finding optimal permutation order $\pi = [\pi(1), \ldots, \pi(U+V)]$. Denote $\boldsymbol{g}_i \in \mathbb{R}^3$ as the waypoint inside the sphere for Super-CH i, $i \in \mathcal{U}$. Then, the traveling time required by the Ferry UAV is

$$T_{\rm tr}(\{\boldsymbol{g}_i\}, \pi) = \frac{\sum_{i=1}^{K-1} \|\boldsymbol{g}_{\pi(i+1)} - \boldsymbol{g}_{\pi(i)}\| + \|\boldsymbol{g}_{\pi(K)} - g_{\pi(1)}\|}{V_{\max}}. \tag{29}$$

Correspondingly, problem (P2) is converted to

$$\begin{aligned} (\text{P2.1}) \quad & \min_{\{\boldsymbol{g}_i\}, \pi} \quad T_{\rm tr}(\{\boldsymbol{g}_i\}, \pi) \\ & \text{s.t.} \quad \|\boldsymbol{g}_i - \boldsymbol{s}_i\| \leqslant r, \quad i \in \mathcal{U}. \end{aligned} \tag{30}$$

Referring to [29], problem (P2.1) is NP-hard, but we can efficiently obtain its suboptimal solution by standard convex optimization techniques with letting $\pi = \hat{\pi}$.

On basis of Cases 1 and 2, for a given flight time T, the initial trajectory of Ferry UAV can be designed as Algorithm 3. According to [29], the corresponding computation complexity is $O(K^{3.5})$.

Algorithm 3 Initial trajectory design for given T

Input: A given T, locations of Super-CHs $\{\boldsymbol{s}_i\}$.
Output: r, the initial trajectory.
Solve TSP to obtain minimum traveling time $T_{\rm tsp}$ and optimal visiting order $\hat{\pi}$ based on $\{\boldsymbol{s}_i\}$;
if $T \geqslant T_{\rm tsp}$ **then**
  Design initial trajectory based on Case 1;
else
  Let $r_l = 0$, r_u be sufficiently large and tolerance $\epsilon > 0$;
  while $|T_{\rm tr} - T| \leqslant \epsilon$ **do**
    $r = (r_l + r_u)/2$;
    Solve problem (P2.1) with visiting order $\hat{\pi}$ to derive traveling time $T_{\rm tr}$ and waypoints $\{\boldsymbol{g}_i\}$;
    if $T_{\rm tr} > T$ **then**
      Let $r_l = r$;
    else
      Let $r_u = r$;
    end if
  end while
  Construct the initial trajectory based on $\{\boldsymbol{g}_i\}$;
end if

5 Numerical simulations

In this section, numerical examples are carried out to evaluate the performance of our proposed approaches. We first apply the modified k-means algorithm in Algorithm 1 to choose one Super-CH UAV in each area, and then utilize the BCD based algorithm in Algorithm 2 to design the optimal 3D trajectory of the Ferry UAV based on positions of selected Super-CHs.

5.1 Clustering and the Super-CH selection

Assume that all UAVs are divided into $K = 6$ areas based on the geographic location, and there are respectively $\{100, 120, 140, 160, 180, 200\}$ UAVs to collect data from the grounds in each area. Within each area, these UAVs are randomly and uniformly distributed. Meanwhile, the packet size is set to $m = 1024$ bits, and the transmission rate of each UAV is $\mu = 10$ Mbps.

According to the numbers of UAVs in areas 1 to 6, we first obtain the optimal numbers of CHs in areas 1 to 6 as $\{10, 11, 12, 13, 13, 14\}$ from Eq. (5). By implementing the modified k-means algorithm in Algorithm 1, the obtained clustering result of each area is depicted in Figure 2. The corresponding locations of 6 super CHs in areas 1 to 6 are

$$\begin{pmatrix} 971 & 3067 & 5976 & 9009 & 5048 & 2023 \\ 2006 & 3032 & 3968 & 5937 & 8966 & 6939 \\ 80 & 563 & 126 & 1106 & 390 & 156 \end{pmatrix},$$

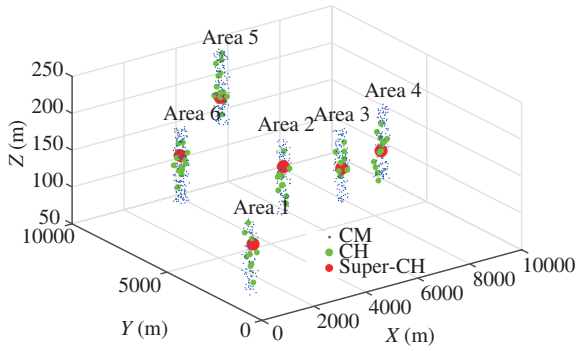

Figure 2 (Color online) Clustering of large-scale UAV swarms.

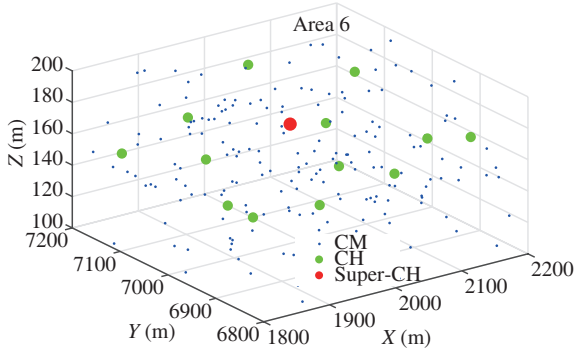

Figure 3 (Color online) Clustering of UAV swarms in area 6.

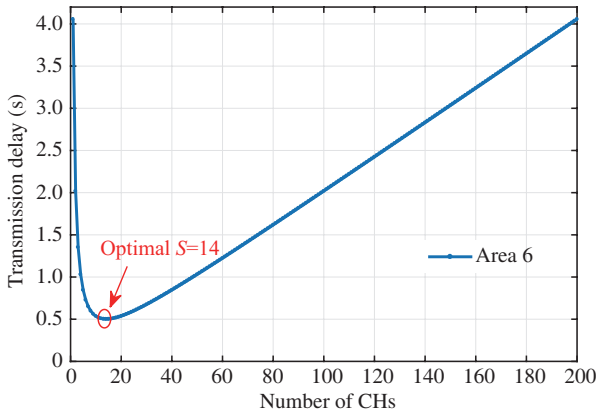

Figure 4 (Color online) Transmission delay with different numbers of CHs in area 6.

where the i-th column represents the location of the Super-CH in area i. Notably, in order to clearly show the clustering results of 6 areas in one figure, we remove the altitude difference among them. The blue dots represent the CMs, green dots represent the CHs, and red dots represent the Super-CHs in areas 1–6. Intuitively, since UAVs are randomly and uniformly distributed in each area, the Super-CH is better to lie at the center of each area for gathering data. As can be seen from Figure 2, each Super-CH approximately lies at the center of each area, which is consistent with the intuition.

In particular, for clarity, we detailedly illustrate the clustering results of UAV swarms of area 6 in Figure 3 as an example. We can clearly observe that each CH is uniformly distributed among CMs, while the Super-CH is almost at the center of area 6. It is responsible for gathering data of the total area where all UAVs are randomly and uniformly distributed.

Moreover, in order to show the effect of the number of CHs versus the transmission delay, we also plot the transmission delay with different number of CHs in area 6 as an example. It is easily seen from Figure 4 that the optimal number of CHs is consistent with the theoretical results $S = 14$.

5.2 3D trajectory optimization

After the locations of Super-CHs are obtained, we will design the 3D optimal trajectory for the Ferry UAV according to positions of selected Super-CHs. The main simulation parameters of this subsection are listed in the following Table 2.

The locations of Super-CHs are shown in Figure 5(a) with Super-CH i being the Super-CH in area i, $i = 1, ..., 6$. We suppose that all Super-CHs have equal throughout requirement, i.e., $C = C_i$, $i \in \mathcal{U}$. In our simulation experiments, we will consider two cases with small and large throughout requirements, which correspond to $C = 300$ and $C = 1500$ Mbits, respectively. For comparison, we also design the optimal 2D trajectory of Ferry UAV with the fixed altitude equal to the maximum height of Super-CH UAVs plus the minimum safe distance $d_{\min}$. When designing an initial trajectory, by solving the corresponding TSP with Super-CHs' locations obtained in Subsection 5.1, we can obtain that the minimum traveling time

Table 2 Main simulation parameters

Parameter	Value	Parameter	Value
Total bandwidth: B	10 MHz	Minimum safe distance between the Ferry UAV and Super-CH UAVs: $d_{\min}$	50 m
Noise power spectrum density: N_0	-169 dBm/Hz	Time step length: δ	4 s
Channel power gain at the reference distance of $d_0 = 1$ m: λ_0	-50 dB	Thresholds in Algorithm 2: ϵ_1, ϵ_2	10^{-2}
Transmit power of each Super-CH: P_i	10 dB	Threshold in Algorithm 3: ϵ	10^{-3}
Maximum speed of the Ferry UAV: $V_{\max}$	50 m/s		

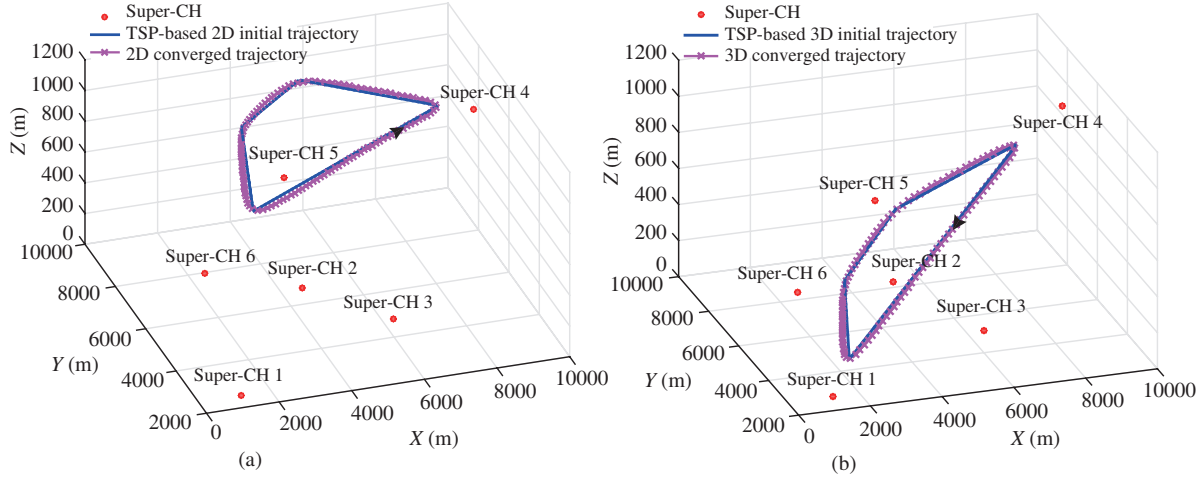

Figure 5 (Color online) Ferry UAV trajectories with throughput requirement $C = 300$ Mbits. (a) Optimal 2D trajectory with fixed altitude; (b) optimal 3D trajectory.

under TSP T_{tsp} are 459 and 453 s for 2D and 3D trajectory optimization, respectively. Meanwhile, the optimal visiting order $\hat{\pi}$ are $[3, 4, 5, 6, 1, 2, 3]$ and $[4, 3, 2, 1, 6, 5, 4]$ in 2D and 3D cases, respectively.

First, when the throughput requirement for each Super-CHs is set as $C = 300$ Mbits, the optimal 3D trajectory and the optimal 2D trajectory together with their corresponding TSP based initialization are depicted in Figure 5. As can be seen from Figure 5, for low rate requirement, the Ferry UAV can complete the data collection without having to reach each Super-CH. The corresponding minimized completion time of optimal 2D and 3D trajectories are obtained as 350 and 319 s, respectively. Therefore, our proposed 3D trajectory optimization is superior to 2D trajectory optimization with fixed altitude.

When the throughput requirement increases to $C = 1500$ Mbits, we display the optimal 3D trajectory, optimal 2D trajectory and their corresponding TSP based initialization in Figure 6. As shown in Figure 6, the Ferry UAV needs to arrive at each Super-CH to meet the throughput requirement. The corresponding completion time of optimal 2D and 3D trajectories for the TSP based trajectory initialization are 1018 and 469 s, respectively. Hence, the 3D trajectory optimization also admits better performance than the 2D trajectory optimization.

Furthermore, for 2D and 3D trajectory optimizations, Figure 7 illustrates the mission completion time with different throughput requirements. We can observe that, the mission completion time for the 3D trajectory is always shorter than that of the 2D trajectory. Therefore, our proposed 3D optimal trajectory design admits better performance than the 2D optimal trajectory design. In particular, when the throughput requirement gets larger, the performance improvement of the 3D trajectory optimization is more obvious compared with the 2D trajectory optimization.

6 Conclusion

In this paper, we have studied a low latency clustering and 3D trajectory design for the large-scale UAV swarms, where numerous UAVs collect data from the ground and the Ferry UAV gathers all UAVs' data together. Specifically, we have divided the UAV swarms into multiple areas based on the geographic location. To facilitate the Ferry UAV's data collection, we have selected a single Super-CH in each area to

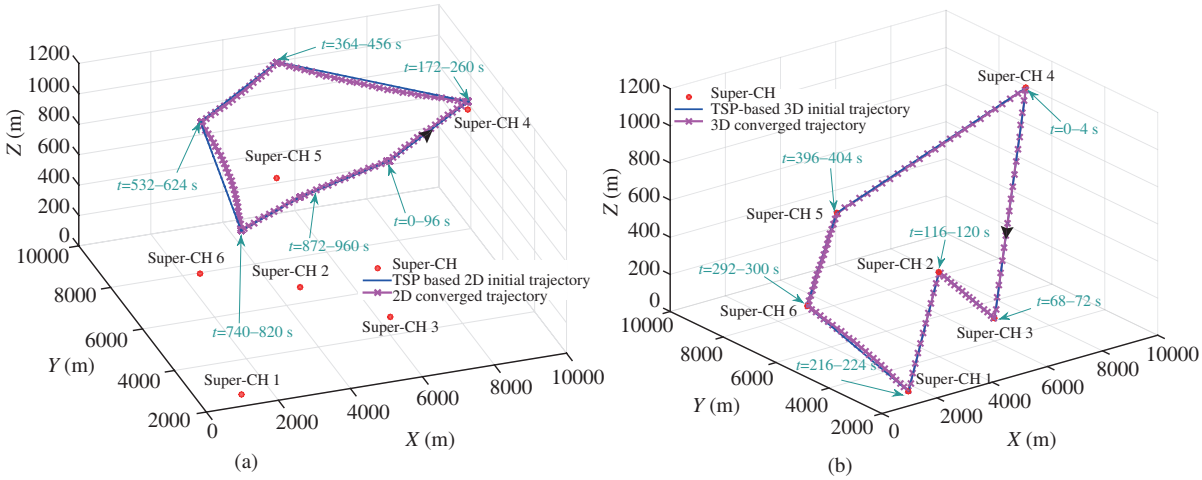

Figure 6 (Color online) Ferry UAV trajectories with throughput requirement $C = 1500$ Mbits. (a) Optimal 2D trajectory with fixed altitude; (b) optimal 3D trajectory.

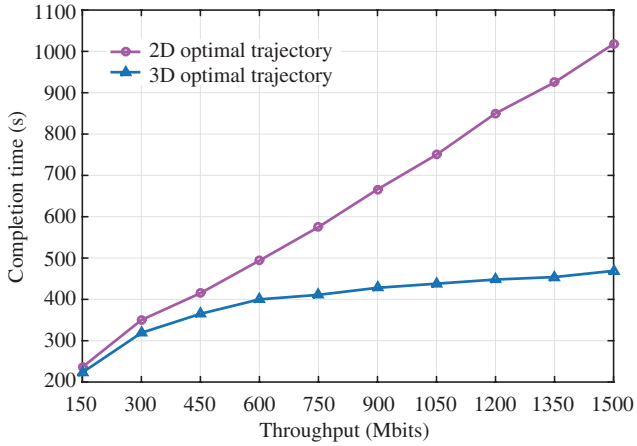

Figure 7 (Color online) Completion time with different throughputs.

gather all data of the area, and thereby the Ferry UAV only needs to collect data from several Super-CH UAVs. Specifically, we have first determined the number of CHs by optimizing the transmission delay, and then applied a modified k-means algorithm to select corresponding CHs as well as the unique Super-CH among CHs in each area. Subsequently, we have proposed a BCD-based iterative approach to design the optimal 3D trajectory of the Ferry UAV such that its completion time of data collection from Super-CHs could be minimized. Numerical simulations show that, the low latency clustering and the modified k-means algorithm can efficiently select Super-CHs, while the proposed 3D trajectory optimization of the Ferry UAV is superior to the 2D trajectory optimization with fixed altitude. For the future work, we will consider the spectrum sharing and coordination between aerial UAVs and ground BSs for the large-scale UAV swarms in 5G and beyond wireless networks.

Acknowledgements This work was supported in part by National Natural Science Foundation of China (Grant No. 61871211), Natural Science Foundation of Jiangsu Province Youth Project (Grant No. BK20180329), Innovation and Entrepreneurship of Jiangsu Province High-level Talent Program, Summit of the Six Top Talents Program of Jiangsu Province.

References

1 Boccardi F, Heath R W, Lozano A, et al. Five disruptive technology directions for 5G. IEEE Commun Mag, 2014, 52: 74–80
2 Zhou H B, Wu Y M, Hu Y Q, et al. A novel stable selection and reliable transmission protocol for clustered heterogeneous wireless sensor networks. Comput Commun, 2010, 33: 1843–1849
3 Ma T, Qian B, Niu D B, et al. A gradient-based method for robust sensor selection in hypothesis testing. Sensors, 2020, 20: 697
4 Shi W S, Zhou H B, Li J L, et al. Drone assisted vehicular networks: architecture, challenges and opportunities. IEEE Netw, 2018, 32: 130–137
5 Cheng N, Xu W C, Shi W S, et al. Air-ground integrated mobile edge networks: architecture, challenges, and opportunities. IEEE Commun Mag, 2018, 56: 26–32

6 Shi W S, Li J L, Xu W C, et al. Multiple drone-cell deployment analyses and optimization in drone assisted radio access networks. IEEE Access, 2018, 6: 12518–12529
7 Zhang S H, Zhang H L, Di B Y, et al. Cellular UAV-to-X communications: design and optimization for multi-UAV networks. IEEE Trans Wirel Commun, 2019, 18: 1346–1359
8 Tuna G, Nefzi B, Conte G. Unmanned aerial vehicle-aided communications system for disaster recovery. J Network Comput Appl, 2014, 41: 27–36
9 Zeng Y, Wu Q Q, Zhang R. Accessing from the sky: a tutorial on UAV communications for 5G and beyond. Proc IEEE, 2019, 107: 2327–2375
10 Matolak D W, Sun R Y. Unmanned aircraft systems: air-ground channel characterization for future applications. IEEE Veh Technol Mag, 2015, 10: 79–85
11 Khawaja W, Guvenc I, Matolak D W, et al. A survey of air-to-ground propagation channel modeling for unmanned aerial vehicles. IEEE Commun Surv Tut, 2019, 21: 2361–2391
12 Shi W S, Li J L, Cheng N, et al. Multi-drone 3-D trajectory planning and scheduling in drone-assisted radio access networks. IEEE Trans Veh Technol, 2019, 68: 8145–8158
13 Zhao N, Lu W D, Sheng M, et al. UAV-assisted emergency networks in disasters. IEEE Wirel Commun, 2019, 26: 45–51
14 Hayat S, Yanmaz E, Muzaffar R. Survey on unmanned aerial vehicle networks for civil applications: a communications viewpoint. IEEE Commun Surv Tut, 2016, 18: 2624–2661
15 Bujari A, Palazzi C E, Ronzani D. FANET application scenarios and mobility models. In: Proceedings of the 3rd Workshop on Micro Aerial Vehicle Networks, Systems, and Applications, NewYork, 2017. 43–46
16 Park J H, Choi S-C, Hussen H R, et al. Analysis of dynamic cluster head selection for mission-oriented flying ad hoc network. In: Proceedings of the 9th International Conference on Ubiquitous and Future Networks (ICUFN), Milan, 2017. 21–23
17 Du J M, You Q D, Zhang Q, et al. A weighted clustering algorithm based on node stability for ad hoc networks. In: Proceedings of the 16th International Conference on Optical Communications and Networks (ICOCN), Wuzhen, 2017
18 Fahad M, Aadil F, Rehman Z, et al. Grey wolf optimization based clustering algorithm for vehicular ad-hoc networks. Comput Electrical Eng, 2018, 70: 853–870
19 Khan A, Aftab F, Zhang Z. BICSF: bio-inspired clustering scheme for FANETs. IEEE Access, 2019, 7: 31446–31456
20 Aadil F, Raza A, Khan M, et al. Energy aware cluster-based routing in flying Ad-Hoc networks. Sensors, 2018, 18: 1413
21 Ali H, Shahzad W, Khan F A. Energy-efficient clustering in mobile ad-hoc networks using multi-objective particle swarm optimization. Appl Soft Comput, 2012, 12: 1913–1928
22 Zhu X P, Bian C J, Chen Y, et al. A low latency clustering method for large-scale drone swarms. IEEE Access, 2019, 7: 186260–186267
23 Zeng Y, Zhang R, Lim T J. Throughput maximization for UAV-enabled mobile relaying systems. IEEE Trans Commun, 2016, 64: 4983–4996
24 Wu Q Q, Zhang R. Common throughput maximization in UAV-enabled OFDMA systems with delay consideration. IEEE Trans Commun, 2018, 66: 6614–6627
25 Zhang G C, Wu Q Q, Cui M, et al. Securing UAV communications via joint trajectory and power control. IEEE Trans Wirel Commun, 2019, 18: 1376–1389
26 Jeong S, Simeone O, Kang J. Mobile edge computing via a UAV-mounted cloudlet: optimization of bit allocation and path planning. IEEE Trans Veh Technol, 2018, 67: 2049–2063
27 Wu Q Q, Zeng Y, Zhang R. Joint trajectory and communication design for multi-UAV enabled wireless networks. IEEE Trans Wirel Commun, 2018, 17: 2109–2121
28 Zhang G C, Wu Q Q, Cui M, et al. Securing UAV communications via trajectory optimization. In: Proceedings of IEEE Global Communications Conference, Singapore, 2017
29 Zhang J W, Zeng Y, Zhang R. UAV-enabled radio access network: multi-mode communication and trajectory design. IEEE Trans Signal Process, 2018, 66: 5269–5284
30 Zhang J, Zhou L, Zhou F H, et al. Computation-efficient offloading and trajectory scheduling for multi-UAV assisted mobile edge computing. IEEE Trans Veh Technol, 2020, 69: 2114–2125
31 Mahajan M, Nimbhorkar P, Kasturi R. The planar k-means problem is NP-hard. Theor Comput Sci, 2009, 442: 274–285
32 Matolak D W, Sun R. Air-ground channel characterization for unmanned aircraft systems-part I: methods, measurements, and models for over-water settings. IEEE Trans Veh Technol, 2017, 66: 26–44
33 Grant M, Boyd S, Ye Y. CVX Toolbox. Redwood City: Stanford University Press, 2009
34 Qian B, Zhou H B, Lyu F, et al. Toward collision-free and efficient coordination for automated vehicles at unsignalized intersection. IEEE Int Things J, 2019, 6: 10408–10420
35 Laporte G. The traveling salesman problem: an overview of exact and approximate algorithms. Eur J Oper Res, 1992, 59: 231–247

Appendix A Proof of Lemma 2

The proof of Lemma 1 is quite similar to that of Proposition 1 in [29]. Let $f(z) = \log_2(1 + \frac{c}{z})$ with $c = \frac{P_i \gamma_0}{\alpha_i^l[n]} > 0$. It is not difficult to verify that $f(z)$ is a convex function with $z \geqslant 0$. Then, $f(z)$ can be globally lower-bounded by its first-order Tayler expansion at any point z_0[1)]. That is, we have

$$f(z) \geqslant f(z_0) + f'(z_0)(z - z_0), \quad \forall z, \tag{A1}$$

where

$$f'(z_0) = \frac{-c \log_2 e}{z_0(z_0 + c)}.$$

Consequently, letting $z = \max(\|\boldsymbol{q}[n] - \boldsymbol{s}_i\|^2, d_{\min}^2)$ and $z_0 = \max(\|\boldsymbol{q}^l[n] - \boldsymbol{s}_i\|^2, d_{\min}^2)$, it completes the proof.

Appendix B Proof of Lemma 3

Recalling the expression of $\hat{R}_i[n]$ in (23), only the term $-\phi_i^l[n] z_i[n]$ involves $\boldsymbol{q}[n]$. We can easily obtain the convexity of $z_i[n] = \max(\|\boldsymbol{q}[n] - \boldsymbol{s}_i\|^2, d_{\min}^2)$ as the maximum of convex function $\|\boldsymbol{q}[n] - \boldsymbol{s}_i\|^2$ and a constant $d_{\min}^2$. Combined with $-\phi_i^l[n] < 0$, it immediately yields the concavity of $-\phi_i^l[n] z_i[n]$ as well as $\hat{R}_i[n]$.

1) Boyd S, Vandenberghe L. Convex Optimization. Cambridge: Cambridge University Press, 2004.